Struct Multidisc Optim (2009) 39:311–325
DOI 10.1007/s00158-008-0327-3

INDUSTRIAL APPLICATION

System reliability based vehicle design for crashworthiness and effects of various uncertainty reduction measures

Erdem Acar · Kiran Solanki

Received: 22 July 2008 / Revised: 23 September 2008 / Accepted: 8 October 2008 / Published online: 31 October 2008

Abstract Reliability-based design optimization of automobile structures for crashworthiness has been studied by many researchers by using either single component probabilistic constraints or single failure mode based probabilistic constraints, while system reliability considerations are mostly disregarded. In this paper, we perform system reliability based design optimization (SRBDO) of an automobile for crashworthiness and analyze the effect of reliability allocation in different failure modes. In addition, effects of various uncertainty reduction measures (e.g., reducing variability in material properties, reducing error of finite element analysis) are investigated and tradeoff plots of uncertainty reduction, system reliability and structural weight are generated. These types of tradeoff plots can be used by a company manager to decide whether to allocate the company resources for employing uncertainty reduction measures or allocating the resources for the excess weight to protect against the unreduced uncertainties. Furthermore, relative importance of automobile structural members in different crash scenarios is quantified.

Submitted for publication in the Structural and Multidisciplinary Optimization (SMO).

E. Acar (✉)
Department of Mechanical Engineering,
TOBB University of Economics and Technology,
Sogutozu, Ankara 06560, Turkey
e-mail: acar@etu.edu.tr

K. Solanki
Center for Advanced Vehicular Systems,
Mississippi State University,
Mississippi State, MS 39762, USA
e-mail: kns3@cavs.msstate.edu

Keywords Automobile crashworthiness · System reliability · Uncertainty reduction · Weight saving

1 Introduction

The computer-aided design (CAD) and the computer-aided engineering (CAE) has been significantly improved over the years to help companies to produce better products. Automotive manufacturers have invested a lot, especially in crashworthiness analysis, to have the ability to design better products in less time and at lower costs. The availability of CAD and CAE products led to application of optimization techniques to automotive structural design by many researchers including Yang et al. (1994, 2000a, b), Esat (1999), Gu et al. (2001), Kodiyalam and Sobieszczanski-Sobieski (2001), Kim et al. (2002), Wang et al. (2003), Lee et al. (2004), Fang et al. (2005), Kaya (2006), and Sinha et al. (2007)

In design of automobiles, crashworthiness considerations are particularly important. Since crash simulations with acceptable accuracy are computationally very expensive, metamodels (or surrogate models) are effectively used in most crashworthiness design and optimization applications. Many researchers compared different metamodels to approximate the crash responses of their interest (e.g., intrusion distance, energy absorption, acceleration, contact force) and each found a different metamodel worked best for their problem. For instance, Yang et al. (2000b) and Gu et al. (2001) recommended the use of second order polynomial regression model and moving least square regression, while Kurtaran et al. (2002) found

the successive response surface approximations to be the most effective. Hamza and Saitou (2004) suggested the use of radial basis neural networks and Fang et al. 2005 recommended radial basis functions, while Stander et al. (2004) found neural networks and Kriging had better accuracy. As seen, there is no solid answer to question of what metamodel is the best for crashworthiness applications. Therefore, in this paper, we try three different metamodels: (1) polynomial response surface approximation, (2) radial basis functions, and (3) Gaussian process metamodels. Then, we select the most accurate metamodel type for the responses of interest.

The uncertainties in design, implementation, manufacturing and operating conditions necessitate the use of design under uncertainty techniques, the most popular technique being the reliability-based design optimization (RBDO). However, since RBDO requires the evaluation of probabilistic constraints many times throughout the optimization, it is computationally expensive. Successful use of metamodeling methods in predicting critical crash responses, on the other hand, opened door for performing RBDO studies, since crash responses can now be estimated in matter of seconds by the use of metamodels. Some earlier work in this area includes the studies of Piskie and Gioutsos (1992), Marvis and Bandte (1997), Yang et al. (2000b, 2002), Gu et al. (2001). More recent RBDO for crashworthiness studies includes the following works. Youn et al. (2004) performed RBDO of a full vehicle system by using performance measure approach and hybrid mean value method while utilizing the response surfaces generated by Gu et al. (2001). Sinha (2007) used approximate moment approach and reliability index approach for reliability calculation and response surfaces generated by Gu et al. (2001) for critical responses to perform multi-objective crashworthiness optimization. Rais-Rohani et al. (2006) conducted RBDO of the side rails of an automobile, where they used advanced mean value plus (AMV+) method to calculate probabilistic constraints while making use of RBF for approximating the critical crash responses. The aforementioned works either used single component probabilistic constraints or single failure mode based constraints. This paper, on the other hand, uses system reliability constraints.

The traditional reliability based design relies on living with the uncertainties and allocating the resources for overdesigned products (e.g., thicker structures) to protect against uncertainties. Instead, the resources can be allocated for some measures to reduce uncertainties (e.g., quality control measures that reduces variability in material properties), which would in turn increase the product safety. Qu et al. (2003) showed that applying a quality control measure that can detect bad designs below two-sigma (i.e., below two standard deviations) can increase the safety of composite panels by three orders of magnitude. Alternatively, the potential of increased safety can be traded for improved performance. That is, instead of increasing the product safety to very high levels, the safety can be kept at its nominal value, while the product performance can be improved. Acar et al. (2006) analyzed the effect of improved failure models on the uncertainty of fracture toughness predictions for sandwich panels. It was shown that improved failure models can reduce the coefficient of variation of fracture toughness predictions from 22% to 15%. This reduction indicated that a small percentage of the designs could be used in more relaxed operation conditions, while most of the designs could be used for harsher operating conditions. In this paper, we aim to investigate the effects of uncertainty reduction measures (URMs) on improving the system reliability, which can also be traded for structural weight saving.

This paper has following main unique contributions. First, system reliability-based crashworthiness optimization is performed and allocation of reliability in different failure modes of the automobile structural components is analyzed. Second, the effects of reducing uncertainty are investigated and tradeoff plots of uncertainty reduction, system reliability improvement and weight savings are generated. These types of plots along with appropriate cost models can be used by a company manager to decide whether to allocate the company resources for employing URMs (e.g., tighter quality control, improved structural analysis models) or allocating the resources for the excess weight to protect against the unreduced uncertainties. Third, the sensitivities of crashworthiness responses and system reliability are analyzed in detail and relative importance of the structural members in different crash scenarios is quantified.

The remainder portion of the paper is organized as follows. Section 2 discusses the details of the crashworthiness analysis and critical responses. Section 3 presents metamodel construction for critical responses. Section 4 discusses system reliability based optimization for crashworthiness. Section 5 presents the results of the sensitivity analysis of the critical responses, the system reliability, as well as results of system reliability-based optimization and effects of various URMs. The paper culminates with the concluding remarks listed in Section 6.

Table 1 Summary of the features of the FEA models

Item	Vehicle model	Barrier model	
		Full frontal	Side
Component	328	N/A	23
Node	320,872	N/A	232,984
Shell element	546,812	N/A	54,761
Solid element	30,649	N/A	192,174
Beam element	63	N/A	0
Total mass (kg)	1,210	N/A	1,388

2 Crashworthiness analysis and critical responses

As noted earlier, crashworthiness considerations are particularly important in safety design of automobiles. An automobile is designed such that the impact energy in a possible crash scenario needs to be absorbed through structural deformation, while the intrusion distances of some structural elements must be smaller than their tolerable values. The selection of the structural elements is based on an earlier study of one of the authors (Fang et al. 2005). In this paper, we consider two crash scenarios: (a) full-frontal impact (FFI), and (b) side impact (SI), whereas other possible scenarios such as offset-frontal impact, roof crash and rear impact are not included. In these two crash scenarios, the energy absorption of the selected structural elements and the intrusion distances of the selected structural elements are taken as critical responses. That is, we have four critical responses of interest: (1) energy absorption of the selected structural elements in FFI scenario, (2) intrusion distances of the selected structural elements in FFI, (3) energy absorption of the selected structural elements in SI scenario, (4) intrusion distances of the selected structural elements in SI.

In this study, we used a single full-scale finite element analysis (FEA) model of a 1996 Dodge Neon in simulations of full frontal, and side impacts. The model was originally developed at the US National Crash Analysis Center (Zaouk et al. 2000a, b) and used by other researchers (Horstemeyer et al. 2004; Fang et al. 2005). The FEA model has detailed meshes of 328 components that consist of 320,872 nodes and 577,524 elements. Approximately 95% of the elements were shell elements. The total vehicle mass is 1,210 kg. As noted earlier, we use this unified model in simulating two types of impacts, FFI in which the vehicle impacted a rigid wall in the front and SI in which a moving deformable barrier (MDB) impacted the vehicle from the side. The MDB model in SI has a mass of 1,388 kg and consists of 232,984 nodes and 246,935 elements with 78% being solid elements. Combining the FEA models of the vehicle and MDB, the model for SI has 553,856 nodes and 824,459 elements. Details of the FFI and SI models are given in Table 1 and the two FE models are illustrated in Fig. 1.

A simulation of 100 ms FFI using LS-DYNA MPP v970 takes approximately 17 h with 36 processors on an IBM Linux Cluster with Intel Pentium III 1.266 GHz processors and 607.5 GB RAM. A simulation of 100 ms SI takes approximately 29 h with the same condition as that of the FFI simulation. The initial speed for FFI and SI is set to 35 mph. Figure 2 illustrates in detail of the test configurations for FFI and SI.

2.1 Design variables

Safety performance of a vehicle can be measured by parameters such as intrusion distance, intrusion velocity, peak acceleration, and contact force. These safety parameters are closely related to the vehicle's energy absorption history that consists of both energy absorption capacity and energy absorption rate. The more energy that can be absorbed by the vehicle in the early stage

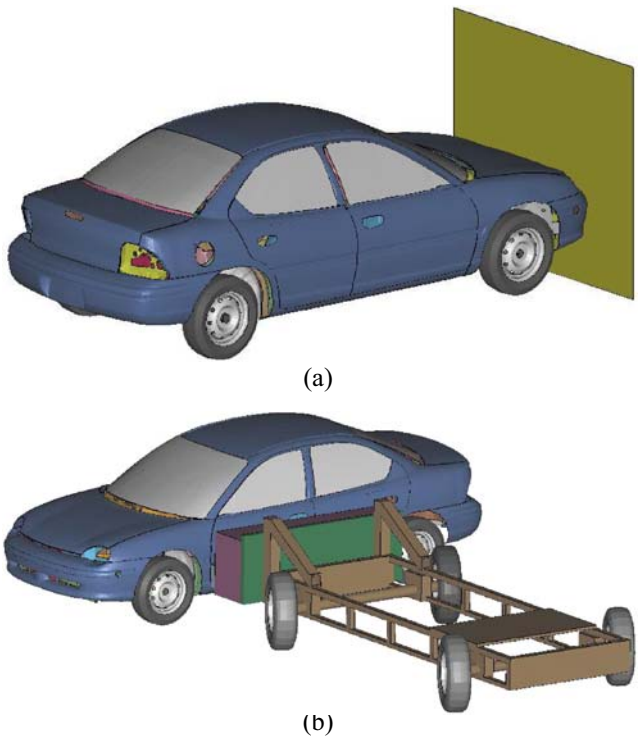

Fig. 1 FE model of a1996 Dodge Neon in two cases of impact scenario **a** full frontal impact, **b** side impact

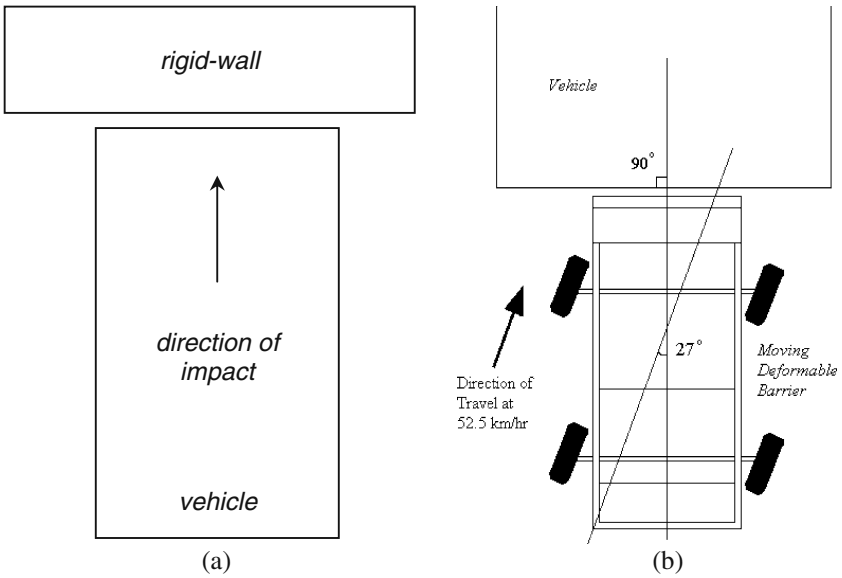

Fig. 2 Plan view of test configurations (not drawn in scale) **a** full frontal impact, **b** side impact

of an impact, the less injury will incur on the occupant. Therefore, an analysis on the energy absorption history will help identifying those important components. The time histories of the vehicle's total strain energies or internal energies for FFI and SI are shown in Fig. 3a and b, respectively.

Since a vehicle impact finishes in a short period (in the magnitude of 100 ms), both the energy absorption capacity and absorption rate are important. A large energy absorption capacity is necessary but not sufficient, because the energy wave passes through a component if the energy cannot be absorbed quickly. Based on this understanding, the energy absorption of all components at 20, 40, and 60 ms were examined in an earlier work of one of the authors (Fang et al. 2005). They selected the structural elements with large energy absorptions in a single or both impacts. In addition, the structural elements with large mass but small or no contribution to the energy absorption were selected for the purpose of mass reduction. A total of 21 structural elements were selected and they are shown in Fig. 4.

Figure 3 shows the time histories of energy absorptions of selected components compared to those of the whole vehicle in FFI and SI. The 21 components account for 45%, 61%, and 61% of the vehicle's total internal energy in FFI at 20, 40, and 60 ms, respectively. They also contribute 45%, 43%, and 43% of the vehicle's total internal energy in SI at 20, 40, and 60 ms, respectively. These contributions are significant considering the fact that the 21 components only hold 8% of the total mass of the vehicle. Table 2 gives the initial mass and thickness of the 21 components. The thicknesses of the selected components are used as design variables for size optimization. A total of 13 design variables were needed for the 21 components due to component symmetry.

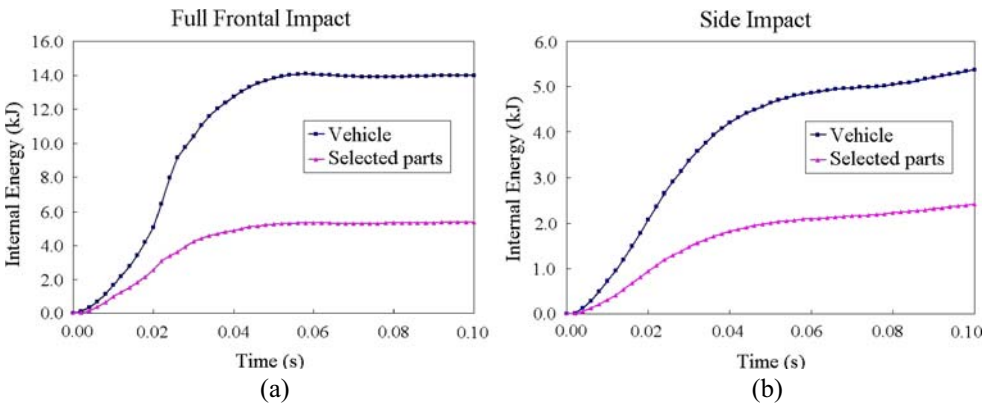

Fig. 3 Time histories of the vehicle's strain energy **a** full-frontal impact, **b** side impact

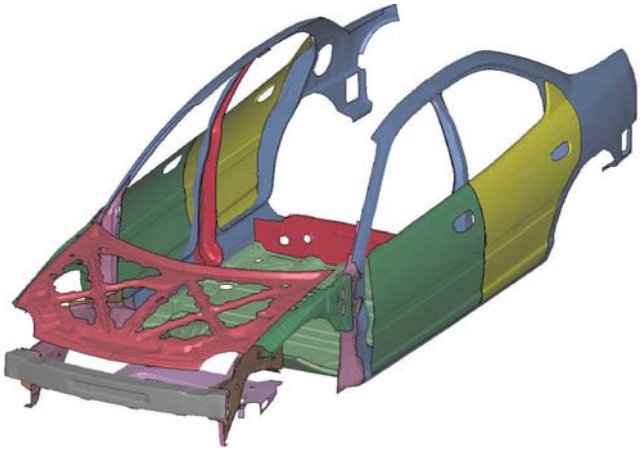

Fig. 4 Selected 21 structural components. There are 13 design variables due to symmetry

In addition to the energy absorption of the selected components, the intrusion distance of the front panel for the case of FFI and intrusion distance of the side door for the cases of SI are also selected as critical responses, because the distance between the front panel and the occupant as well as the distance between the side door and the occupant is very small. For FFI, the average intrusion distance of six points on the front panel is used as a response of our interest. Similarly, the average intrusion distance of 12 points on the door under SI is used as a response of our interest. The approximate locations of these points are illustrated in Fig. 5.

Table 2 The description of the design variables and their initial (or baseline) values

ID number	Design variable	Component	Initial thickness (mm)
V1	DV1	Left and right front doors	0.85
V2	DV2	Left and right rear doors	0.83
V3	DV3	Inner hood	0.65
V4	DV4	Left and right outer B-pillars	1.61
V5	DV5	Left and right middle B-pillar	0.71
V6	DV6	Inner front bumper	1.96
V7	DV7	Front floor panel	0.71
V8	DV8	Left and right outer CBN	0.83
V9	DV9	Left and right front fenders	1.52
V10	DV10	Left and right inner front rails	1.90
V11	DV11	Left and right outer front rails	1.52
V12	DV12	Rear plate	0.71
V13	DV13	Suspension frame	2.61

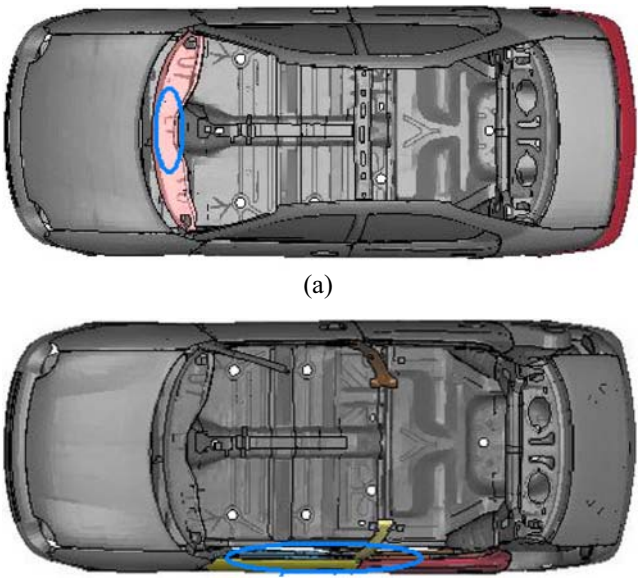

(a)

(b)

Fig. 5 Plan view of approximate locations for intrusion measurement **a** full frontal impact, **b** side impact

2.2 Random variables

Engineering systems contain many different kinds of uncertainties found in material and component structures, computational models, input variables, and constraints. Potential sources of uncertainty in a system include human errors, manufacturing or processing variations, operating condition variations, inaccurate or insufficient data, assumptions and idealizations, and lack of knowledge. Manufacturing variations are manifested as tolerances in part dimensions, missing small sized parts or joints, and porosity in the base material. Operating conditions, such as the ambient temperature and air flowrate, may vary as well. In addition to these sources of uncertainty, the finite element analysis requires for systems behaviour evaluation incorporate a number of simplifying assumptions. Examples include idealized modeling of boundary conditions as well as mesh size. Many of these simplifying assumptions are required in order to make the analyses fast enough for a complex, iterative design process. Since nondeterministic factors in a system sometimes produce considerable variations in predicted system responses, uncertainty is an important factor for designers to consider when making decisions regarding design specifications.

In present study, five random variables are used to introduce uncertainty into the crash simulations: (1) a material uncertainty parameter, (2) the occupant mass, (3) the impact speed, (4) the uncertainty term responsible for error in finite element analysis on predicting the

Table 3 The probability distribution types and the distribution parameters of the random variables

ID#	Random variable	Description	Distribution	Parameters
V14	RV1	Material parameter	Normal	1, 0.1667
V15	RV2	Occupant mass (lb)	Normal	200, 0.1667
V16	RV3	Impact speed (mph)	Normal	35, 0.1667
V17	RV4	Error in FEA	Uniform	−20% , 20%
V18	RV5	Error in our ignorance	Uniform	−10% , 10%

The parameters of the normal distribution are the mean and the coefficient variation, respectively. The parameters of the uniform distribution are the lower and the upper bound, respectively.

crash responses and error in constructed metamodels for the responses, and (5) the error due to excluding some randomness in our analysis (e.g., ignoring uncertainty in impact direction). The probability distribution types and the distribution parameters of the random variables are provided in Table 3. Interpretation of the uncertainties in the occupant mass and the impact speed is fairly obvious, but the other uncertainty terms deserve some explanation as provided in the followings.

2.2.1 Material uncertainty

Since materials are complex, hierarchical, heterogeneous systems, it is not reasonable or sufficient to adopt a deterministic approach to materials design. First, microstructure is inherently random at some scales. Second, parameters of a given model are subject to variation associated with variation of material microstructure from specimen to specimen. Furthermore, variation is associated with the structures and morphologies of realized materials due to variations in processing history and other factors. Figure 6a shows the effect of strain rate on the true stress-strain curve. Often, it is expensive or impossible to remove and measure these sources of variability, but their impact on model predictions and final system performance can be profound. As suggested by Horstemeyer et al. (2005), small variability (∼1%) in microstructures can result in very large (∼13%) variation in failure stress. Here, we incorporate material uncertainty due to microstructural features, manufacturing processes, and their history effects by using an uncertainty stress-strain parameter defined by random variable RV1. This random variable is assumed to have a normal distribution and it describes the variability in the plastic portion of material stress-strain curves, as illustrated in Fig. 6b.

2.2.2 Error in finite element predictions of crashworthiness responses and metamodels

Uncertainty is associated with crash response predictions of finite element analysis. Finite element models inevitably incorporate assumptions and approximations that impact the precision and accuracy of predictions. In addition, the element types used and the mesh size have a profound effect in finite element predictions. Furthermore, in this study these crash responses will be approximated via metamodels during reliability assessment. That brings another layer of uncertainty. In this study, we consider two crash responses of our interest: intrusion distance and energy absorption. For both of the responses, we assume that the uncertainity term responsible for the error in finite element predictions and errors in metamodel approximations is limited to ±20%. This error bound is selected based solely on our experience, and the distribution for the error is assumed to be uniform in order to reflect our lack of prior information on this error term.

2.2.3 Error due to excluding some randomness in crash analysis

Random variables RV1-RV4 are used to introduce uncertainty into crash simulations. Apart from these four random variables, there may exist some other random variables that we treated as deterministic. For instance, in this study we consider two crash scenario of our interest (full frontal impact and side impact) and we assume that the impact direction is straight. That is, we ignored the potential randomness in the impact

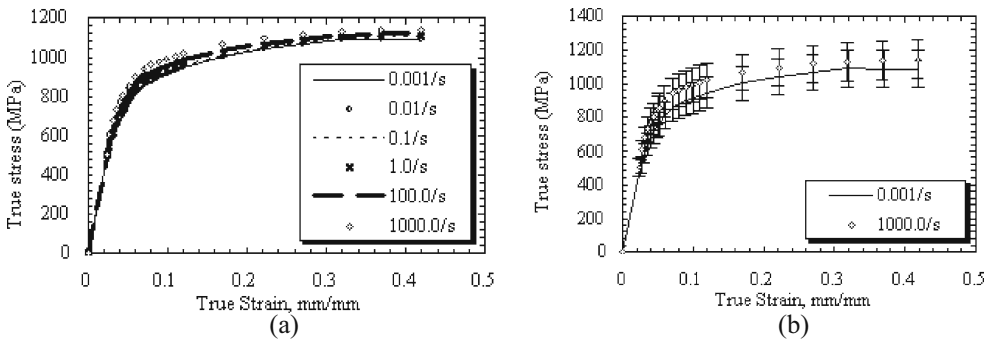

Fig. 6 Effect of strain rate on **a** material constitutive relationship and **b** the band of uncertainty

angle, which may have a significant effect on the crash responses. To compensate for these kinds of ignorance, we introduce an error term, the fifth random variable (RV5), that follows a uniform distribution and bounded by ±10%.

3 Metamodel construction for critical responses and weight

Since crash simulations with acceptable accuracy are computationally very expensive, metamodels are widely used in most crashworthiness optimization applications. The metamodels are used to construct a mathematical relationship between the critical responses of interest as well as the structural weight and the design as well as the random variables. Most commonly used metamodels are: polynomial response surface (PRS) approximations (see Myers and Montgomery 2002), radial basis function (RBF) metamodels (see Dyn et al. 1986; Mullur and Messac 2004), Kriging (see Lophaven et al. 2002; Martin and Simpson 2005), Gaussian process (GP) metamodels (see Wang et al. 2005; Rasmussen and Williams 2006), and support vector regression (see Gunn 1997; Clarke et al. 2005).

In this study, we generate three different types of metamodels for each critical response: quadratic PRS (QPRS), RBF, and GP. For the weight, on the other hand, we only generate linear polynomial response surface (LPRS), because the weight must be linearly related to component thicknesses. We use two different leave-one-out cross validation error metrics to evaluate the accuracies of the metamodels: (1) the mean absolute cross validation error, and (2) the correlation coefficient between the actual and the predicted values of the responses. We find for all the critical responses that GP provide the most accurate predictions. The accuracy evaluations of metamodels are provided in Appendix 1. The constructed metamodels will be used on system reliability calculation as discussed in the next section.

We use the maximin space filling technique proposed by Mourelatos et al. (2006) to generate the necessary training points for the metamodels. In maximin technique, the location of a new point to be added into the design of experiments is selected such that the minimum distance between the points is maximized. We have 13 design variables and three random variables. A quadratic polynomial in terms of 16 variables has 153 coefficients. It is a common practice to choose the number of training points as 1.5–2.0 times the number of coefficients in a quadratic polynomial, so we decided to generate 300 training points.

4 System reliability based optimization

In this section, we first discuss the simple error model used in this study and system reliability estimation. Then, we present two alternative system reliability-based optimization formulations.

4.1 Error model and the system reliability

We use a simple error model that we introduced in our earlier studies (see Acar et al. 2006, 2007). The actual values of the responses of our interest (intrusion distances and energy absorption), R_{act}, and the estimated values of these responses, R_{est}, can be related to each other through

$$R_{\text{est}} = (1 + e)\, R_{\text{act}} \tag{1}$$

where e is the error term. In this study, we have two separate error terms (RV4 and RV5). Thus, we write

$$R_{\text{est}} = (1 + e_1)\,(1 + e_2)\, R_{\text{act}} \tag{2}$$

where e_1 accounts for the error in finite element predictions and the error of metamodel predictions for the responses, and e_2 accounts for the error due to our ignorance of some of the randomness.

We have two critical responses of our interest under two separate crash conditions. Therefore, the system reliability is governed by the consideration of four limit-state functions given in the followings.

$$g_1 = \frac{E_{\text{est}}^{\text{FFI}}}{(1 + e_1)\,(1 + e_2)} - E_{\text{crit}}^{\text{FFI}} \tag{3.1}$$

$$g_2 = D_{\text{crit}}^{\text{FFI}} - \frac{D_{\text{est}}^{\text{FFI}}}{(1 + e_1)\,(1 + e_2)} \tag{3.2}$$

$$g_3 = \frac{E_{\text{est}}^{\text{SI}}}{(1 + e_1)\,(1 + e_2)} - E_{\text{crit}}^{\text{SI}} \tag{3.3}$$

$$g_4 = D_{\text{crit}}^{\text{SI}} - \frac{D_{\text{est}}^{\text{SI}}}{(1 + e_1)\,(1 + e_2)} \tag{3.4}$$

where E is the energy absorbed by the structural components in crash, D is the intrusion distance, the superscripts 'FFI' and 'SI' refers to the full frontal impact and side impact scenarios, the subscript 'est' stands for the estimated value of the response, and the subscript 'crit' refers to the critical values of these responses, which are set to $E_{\text{crit}}^{\text{FFI}} = 89.5\,\text{MPa}$, $D_{\text{crit}}^{\text{FFI}} = 158.5\,\text{mm}$, $E_{\text{crit}}^{\text{SI}} = 28.6\,\text{MPa}$, and $D_{\text{crit}}^{\text{SI}} = 573.7\,\text{mm}$.

The most robust way of computing system reliability is through the Monte Carlo simulation (MCS) method

(Robert and Casella 2004). The correlation between different failure modes is taken care of by itself automatically. Since the existence of metamodels renders the MCS in reliability estimations, we use MCS in system reliability assessment.

4.2 System reliability-based design optimization, SRBDO

Several alternative formulations can be utilized for SRBDO for crashworthiness. For instance, the structural weight can be minimized such that the system reliability can be maintained above a pre-specified target value. In this case, the SRBDO problem can be written as

$$\text{Find } \mathbf{DV} \tag{4.1}$$

$$\text{Min W } (\mathbf{DV}) \tag{4.2}$$

$$\text{Such that } R_S\,(\mathbf{DV}) \leq R_{\text{target}} \tag{4.3}$$

$$\mathbf{DV^L} \leq \mathbf{DV} \leq \mathbf{DV^U} \tag{4.4}$$

where **DV** is the design variable vector, W is the structural weight, R_S is the system reliability, R_{target} is the target reliability that must be ensured, and $\mathbf{DV}^L$ and $\mathbf{DV}^U$ are the lower and the upper bound vectors for the design variables, respectively. In our case, **DV** vector consists of the thicknesses of the selected structural parts, and R_{target} is taken as the system reliability of the baseline design.

Alternatively, one may want to keep the weight of the structure unchanged while maximizing the system reliability via efficient allocation of reliability between different failure modes (see Yang et al. 1999; Ivanovic 2000; Acar and Haftka 2005). In that case, the SRBDO problem can be written as

$$\text{Find } \mathbf{DV} \tag{5.1}$$

$$\text{Min} - R_S\,(\mathbf{DV}) \tag{5.2}$$

$$\text{Such that } W\,(\mathbf{DV}) \leq W_{\text{base}} \tag{5.3}$$

$$\mathbf{DV^L} \leq \mathbf{DV} \leq \mathbf{DV^U} \tag{5.4}$$

where W_{base} is the baseline weight of the vehicle. Here we use normalized value of the weight such that the baseline weight is set to 1.0.

Solution of Eqs. 4.1–4.4 or 5.1–5.4 requires the calculation of the system reliability R_S for many times. Even though the calculation of failure probabilities is not very expensive with the existence of metamodels, we construct metamodels for the system reliability index in terms of the design variables since the metamodels are also useful in sensitivity analysis and can filter out the numerical noise. The system reliability, R_S, and its corresponding reliability index, β_S, are related to each other through

$$\beta_S = \Phi^{-1}\,(R_S) \tag{6}$$

where Φ is the cumulative distribution function of the standard normal distribution.

An FQRS in terms of 13 variables has 105 coefficients, so we use 200 training points while constructing the metamodels for the system reliability index in terms of design variables. We construct three different types of metamodels (QPRS, RBF, and GP) and find that the GP metamodel is the most accurate (similar to the case of the metamodels constructed earlier for the critical responses). The evaluation of accuracies of these different metamodels is provided in Appendix 2. The mean absolute cross validation error is computed as 3.28%, indicating a reasonably good fit. If the error in the metamodels for the reliability index was large, then we would consider using the probabilistic sufficiency factor (PSF) of Qu and Hafka (2004) instead of reliability index, as Qu and Haftka (2004) showed that the metamodels built for PSF could be more accurate than the ones built for reliability index.

5 Results

In this section, we first calculate the sensitivities of the critical responses to the design variables and the random variables. Next, the sensitivities of the system reliability to the design variables are computed and the reliability allocation between different failure modes is explored. Then, SRBDO for crashworthiness is performed. Finally, the effects of reducing uncertainties on the structural safety and weight savings are investigated.

5.1 Sensitivities of the estimated critical responses and the weight

The easiest way of calculating the sensitivities is to fit a LRS to the estimated values of the responses of interest, where the coefficients in the LRS give the sensitivities. Figure 7 shows that for all the critical responses, the impact speed (16th variable) is the most dominant parameter. Figure 8 shows the effect of other variables (than the impact speed) on the critical responses. We see for the FFI scenario that the energy

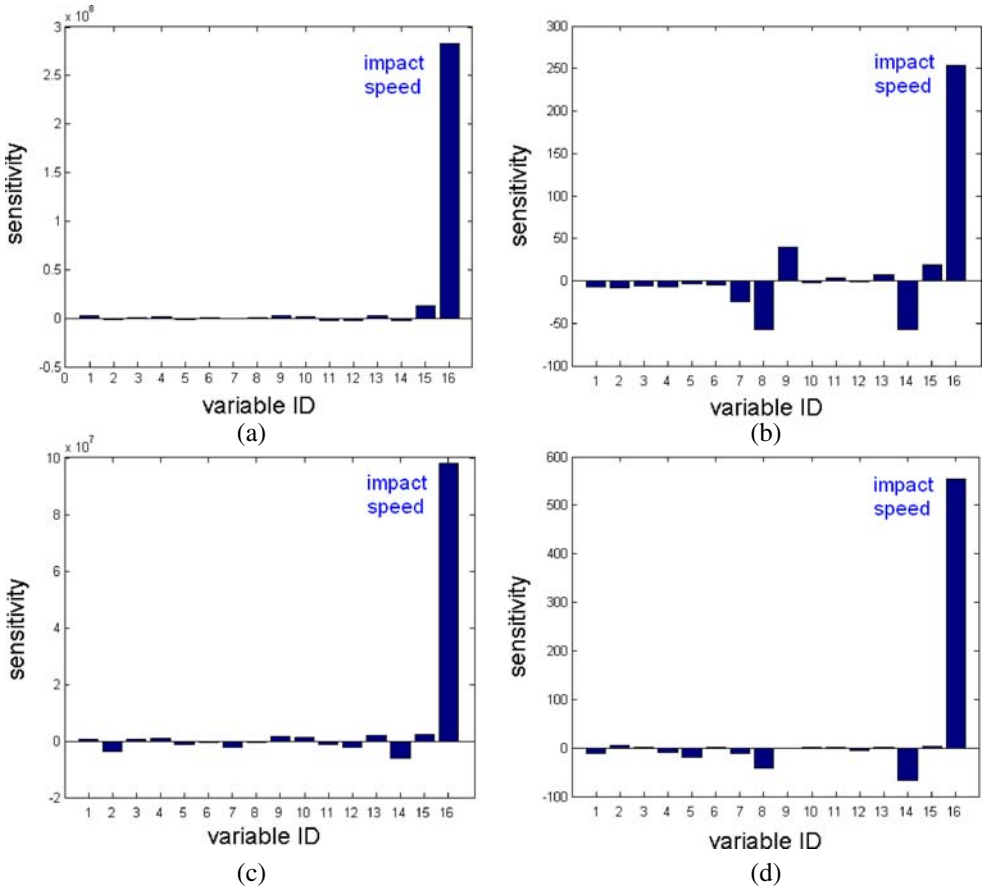

Fig. 7 Sensitivities of the estimated values of the critical responses to the design variables and the random variables

absorption is highly affected by the occupant mass (15th variable) such that as the occupant mass is increased the energy absorption is increased. The intrusion distance in FFI scenario is mainly controlled by the thickness of the left and the right outer CBN (8th variable) and the material uncertainty parameter (14th variable). As the thicknesses of the left and the right outer CBN are reduced, the intrusion distance is increased, which is no surprise. Also, when the material uncertainty parameter takes negative values (that is the material becomes softer), the intrusion distance is increased.

For the SI scenario, the material uncertainty parameter is particularly important. As noted earlier, as the material uncertainty parameter takes negative values, the energy absorption and the intrusion distance in SSI increases. We do not see this behavior in the energy absorption in FFI scenario because in that case the automobile is moving, so the kinetic effects become important that explains the strong dependence to the occupant mass.

5.2 Sensitivities of the system reliability index

To calculate the sensitivity of system reliability, we follow a similar approach as in the previous section. We fit LRS metamodels to the system reliability index, where the coefficients of the LRS metamodel depict the sensitivities.

Figure 9 shows that the overall system reliability is dominated by the following design variables: the thicknesses of the front doors (DV1), the thicknesses of the front floor panels (DV7), the thicknesses of the left and right outer CBN (DV8), and the thicknesses of the left and right front fenders (DV9). Amongst these three parameters, the thickness of the left and right outer CBN (DV8) is the most effective. Figure 10 also shows that increasing the thicknesses of the front floor panel (DV7) and the thicknesses of the left and right outer CBN (DV8), and decreasing the thicknesses of the left and right front fenders (DV9) leads to system reliability improvement.

5.3 System reliability-based design optimization results

The results of RBDO for different failure modes and SRBDO for weight and failure probability minimization are presented in Table 4. The columns 2–5 of Table 4 present the results of RBDO for individual failure modes (RBDO_1 through RBDO_4). In RBDO_1 case, the reliability of energy absorption under FFI is

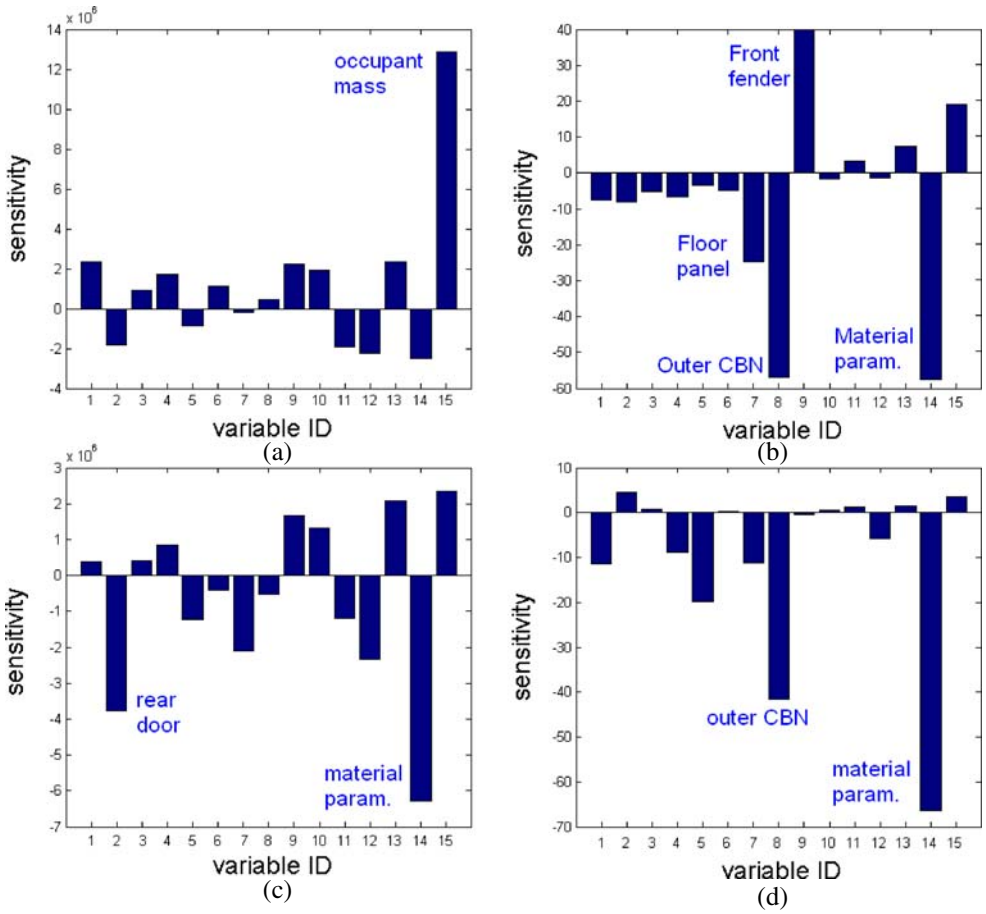

Fig. 8 Sensitivities of the critical responses to the design variables and the random variables when the impact speed is kept constant

maximized, while in RBDO_2 case the reliability of intrusion distance under FFI is maximized. Similarly, in RBDO_3 case, the reliability of energy absorption under SI is maximized, while in RBDO_4 case the reliability of intrusion distance under SI is maximized. The last two columns present the SRBDO results for maximum system reliability (SRBDO_R) and for the minimum weight (SRBDO_W), respectively.

In Table 4, comparison of the column 7 to the columns 3–6 motivates the need for the use of system

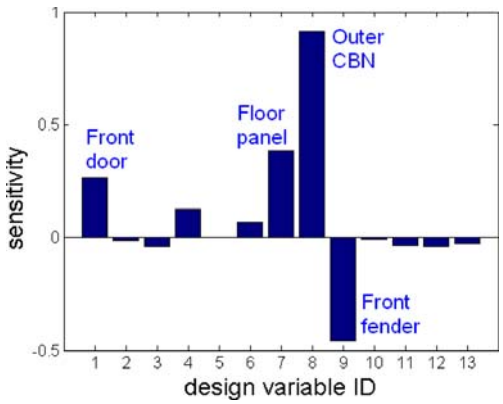

Fig. 9 Sensitivity of the system reliability index to design variables

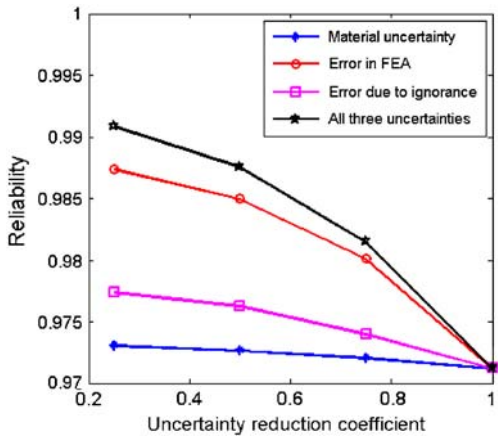

Fig. 10 Effect of uncertainty reduction measures on the system reliability

Table 4 RBDO and SRBDO optimization results

	Baseline	RBDO_1	RBDO_2	RBDO_3	RBDO_4	SRBDO_R	SRBDO_W
DV1	0.5	0.7317	0	1	0	1.0	0
DV2	0.5	1	0	0.7989	0	0.1133	0
DV3	0.5	0	1	1	0	0.0	0
DV4	0.5	1	0.0835	0	1	0.0	0
DV5	0.5	0	0	0	1	0.9373	0
DV6	0.5	1	0.0504	0	0	1.0	0
DV7	0.5	1	0.8398	0	1	0.3332	0
DV8	0.5	0	1	1	1	0.9711	0.7904
DV9	0.5	0.1285	0.0559	0	0.5850	0.4847	0
DV10	0.5	0	0	0	0	0.0	0
DV11	0.5	0	0	1	0	0.0	0.1870
DV12	0.5	1	1	0	0	0.0	0
DV13	0.5	1	0.2220	0.2430	0	0.0	0
R1_MCS	0.9842	**0.9965**	0.9711	0.9855	0.9697	0.9931	0.9791
R2_MCS	0.9902	0.9988	**1.0**	0.9999	1.0	0.9997	0.9961
R3_MCS	0.9862	0.9732	0.9852	**0.9960**	0.9837	0.9949	0.9903
R4_MCS	0.9898	0.9881	0.9983	0.9940	**1.0**	0.9988	0.9917
SR_MCS	0.9712	0.9613	0.9695	0.9799	0.9696	**0.9919**	0.9704
SR_GP	0.9705	0.9718	0.9742	0.9765	0.9865	0.9917	0.9712
Weight	1.0	1.0	0.9940	1.0	1.0	1.0	0.9702

Reliability estimations are performed via MCS with sample size of 100,000. The maximum component reliabilities and the system reliability attained are denoted with bold font

reliability based design optimization. We see that even though none of the individual reliabilities is pushed to its maximum value, the reliabilities of different failure modes are optimally allocated in such a way that the system reliability is maximized. We notice that by redistributing the total structural weight amongst the selected components, the system reliability can be increased from 0.9712 to 0.9919, which is 2.1% improvement. If the reliabilities are converted to probabilities of failure, the conclusion is much stronger such that the system failure probability is reduced from 0.0288 to 0.0081, about 72% reduction! Alternatively, the system reliability can be kept constant and the total structural weight can be reduced. The last column shows that the weight can be reduced from 1.0 to 0.9702, around 3% reduction.

The Gaussian process metamodel predictions of system reliability are compared to MCS estimations (with sample size of 100,000) in Table 4. We notice that the metamodel predictions match well with the MCS predictions when the optimum design is not very close to the boundaries of the design domain (e.g., for RBDO_2 and SRBDO_R). However, the GP prediction is not very accurate for RBDO_4 optimum, which has only one design variable away from the design domain boundary.

5.4 The effect of reducing uncertainties

Recall that we have five random variables: (1) a material uncertainty parameter, (2) occupant mass, (3) impact speed, (4) the uncertainty term responsible for error in finite element analysis on predicting the crash responses and error in constructed metamodels for the responses, and (5) the error due to excluding some randomness in our analysis. Amongst these random variables, we do not have control over the occupant mass and the impact speed, while the other uncertainties can be reduced by employing proper URMs. The material uncertainty can be reduced by measures such

Table 5 Effect of uncertainty reduction on the system reliability of the baseline design

Uncertainty reduction coefficient[a]	Reduction of material uncertainty	Reduction error in FEA	Reduction of error in ignorance	Reduction of all three uncertainty terms
0.75	0.9718	0.9801	0.9740	0.9815
0.50	0.9727	0.9850	0.9763	0.9876
0.25	0.9731	0.9874	0.9774	0.9909

The system reliability of baseline design without any uncertainty reduction is computed as 0.9712 via MCS with sample size of 100,000
[a]The nominal value of the uncertainty is multiplied by this coefficient

Table 6 Effect of uncertainty reduction on the reliability based optimum weight

Uncertainty reduction coefficient[a]	Reduction of material uncertainty	Reduction of error in FEA	Reduction of error in ignorance	Reduction of all three uncertainty terms
0.75	0.9678	0.9620	0.9659	0.9608
0.50	0.9669	0.9597	0.9647	0.9578
0.25	0.9669	0.9580	0.9637	0.9567

[a]The nominal value of the uncertainty is multiplied by this coefficient
The weight of the optimum design with no URM applied is 0.9702. The system reliability of all optimum designs are maintained at 0.9712.

as controlling material process parameters or employing tighter quality control. For instance, in an extrusion process the material uncertainty can be reduced by controlling the process parameters such as the extrusion speed, the temperature and the coefficient of friction between the die and the blank. Similarly, the error in finite element analysis on predicting the crash responses can be reduced by fine meshing or developing more accurate finite element types. The error in constructed metamodels for the responses can be reduced by increasing the number of training points used in building the metamodels or employing better metamodels strategies such as the ensemble of metamodels (see Goel et al. 2007; Acar and Rais-Rohani 2008).

Table 5 and Fig. 10 show the effect of reducing uncertainty on the system reliability of the baseline design. We observe that as the uncertainties are reduced, the system reliability is improved as expected. However, the reliability improvement is more profound at the earlier stages of a URM. That is, the reliability improvement obtained by reducing the uncertainty from its nominal value to 75% of its nominal value is greater than the reliability improvement obtained by reducing the uncertainty from 75% of its nominal value to 50%. We also found that the error reduction was more effective than the variability reduction. The tradeoff plot in Fig. 10 can be utilized by the company manager to decide whether to assign the expenditures for overdesigned (i.e., heavier) structures or assign the expenditures to employ URMs, and if so what type of URM is preferable over the others. For making this kind of a decision, Fig. 10 needs to be accompanied by cost models of structural weight and the URMs as well as structural weight versus URM tradeoff plots, which we will generate next.

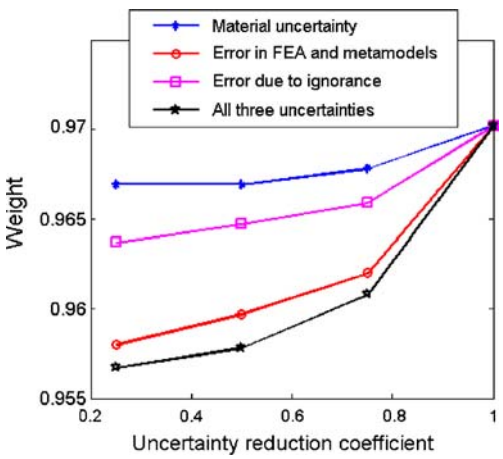

Fig. 11 Effect of uncertainty reduction measures on structural weight

To generate structural weight versus URM tradeoff plots, we perform system reliability based optimization for minimum weight (Eqs. 4.1–4.4) within the presence of URMs. For that purpose, we generate metamodels for the system reliability index when a URM of interest is applied. We consider reduction of three separate uncertainty terms as well as simultaneous reduction of all the terms. The results are presented in Table 6 and Fig. 11. Table 6 shows that application of URMs can increase the weight savings further down to 4.3% (compare to 3% weight saving with no URM). The trend in Fig. 11 is similar to that of Fig. 10 in that as the uncertainties are reduced, more weight can be saved, while the weight saving rate is reduced as uncertainty is reduced further to very small values.

6 Concluding remarks

System reliability-based crashworthiness optimization of an automobile is performed and reliability allocation in different failure modes is analyzed. The effect of various uncertainty reduction measures is evaluated and the tradeoff plots of uncertainty reduction measures, system reliability, and structural weight are generated. These types of tradeoff plots along with proper cost

models can be used by a company manager to decide whether to assign the expenditures to employ URMs (e.g., tighter quality controls, reduced manufacturing variability, improved structural analysis models) or to the excess weight to protect against the unreduced uncertainties. The sensitivity analysis of crashworthiness responses and system reliability are analyzed and relative importance of the structural members in different crash scenarios is quantified. From the results obtained in this study, we drew the following conclusions.

- SRBDO for maximum system reliability did not maximize any of the individual failure probabilities. However, the reliabilities of different failure modes were optimally allocated within the system such that the system failure probability was minimized. The system failure probability could be reduced by 72% for the same weight.
- Similarly, when SRBDO for weight minimization was performed, 3% structural weight saving could be achieved without jeopardizing the overall structural safety.
- Reducing uncertainties greatly improved the system reliability, and the improvement in system reliability was translated into weight savings. We found that as uncertainties are reduced, even though more weight can be saved, the rate of weight saving is reduced.
- For this specific problem, we found that reducing errors was more effective than reducing material uncertainty.
- The most dominant parameter affecting the crash responses of an automobile was found to be the impact speed. The most important design variable influencing the system reliability was the thickness of the outer CBN, followed by the thicknesses of front fenders, floor panels and front doors.

Acknowledgements This study is partially funded by the US Department of Energy under Grant No. DE-FC26-06NT42755 and Center for Advanced Vehicular Systems of the Mississippi State University. These supports are gratefully acknowledged. The authors thank Dr. Raphael T. Haftka for providing his insights into the error model.

Appendix 1 Evaluation of the accuracies of metamodels constructed to approximate the critical system responses and the weight

We generate three types of metamodels: QPRS, RBF, and GP for each critical response and LPRS for the

Table 7 Accuracy of metamodels constructed for energy absorption in full frontal impact

Error metric	QPRS	RBF	GP
% Mean absolute cross validation error	4.50	8.02	2.53
Correlation coefficient	0.9971	0.9930	0.9963

Table 8 Accuracy of metamodels constructed for intrusion distance in full frontal impact

Error metric	QPRS	RBF	GP
% Mean absolute cross validation error	26.64	40.99	13.26
Correlation coefficient	0.9912	0.9828	0.9945

Table 9 Accuracy of metamodels constructed for energy absorption in side impact

Error metric	FQPRS	RBF	GP
% Mean absolute cross validation error	9.74	11.39	2.88
Correlation coefficient	0.9875	0.9833	0.9914

Table 10 Accuracy of metamodels constructed for intrusion distance in side impact

Error metric	FQPRS	RBF	GP
% Mean absolute cross validation error	3.29	3.82	2.14
Correlation coefficient	0.9981	0.9978	0.9985

Table 11 Accuracy of the LPRS metamodel constructed for weight

Error metric	Value
% Mean absolute cross validation error	0.005
Correlation coefficient	0.99998

weight. We use two error metrics to evaluate the accuracies of these metamodels: (1) the mean absolute cross validation error, and (2) the correlation coefficient between the actual and the predicted values of the responses.

The mean absolute cross validation error is an estimator of the global mean absolute error, and it can be calculated from

$$\text{macve} = \frac{1}{N}\sum_{k=1}^{N}\left|\frac{y^k - \hat{y}^{(k)}}{y^k}\right| \tag{A.1}$$

where y^k is the true response at x_k and $\hat{y}^{(k)}$ is the corresponding predicted value from the metamodel constructed using all except the kth design point.

Tables 7, 8, 9 and 10 show that for all the critical responses, the GP metamodels yields the most accurate metamodels. The two error metrics indicate that the accuracies of the metamodels are acceptable. Table 11 shows that the LPRS constructed for structural weight is also very accurate.

Appendix 2 Evaluation of the accuracies of metamodels constructed to approximate the reliability indices for different failure modes

We generate three types of metamodels: QPRS, RBF, and GP for the system reliability index. We use two error metrics to evaluate the accuracies of these metamodels: (1) the mean absolute cross validation error, and (2) the correlation coefficient between the actual and the predicted values. Table 12 shows that for the system reliability index, the GP metamodel is the most accurate.

Table 12 Accuracy of the metamodels built for system reliability index

Error metric	QPRS	RBF	GP
% Mean absolute cross validation error	4.98	7.02	3.28
Correlation coefficient	0.9746	0.9601	0.9858

References

Acar E, Haftka RT (2005) Reliability based aircraft structural design optimization with uncertainty about probability distributions. In: Proceedings of the 6th world congress on structural and multidisciplinary optimization, Rio de Janeiro, Brazil, 30 May–3 June 2005

Acar E, Rais-Rohani M (2008) Enhanced surrogate modeling via optimum ensemble of metamodels. Struct and Multidisc Optim (published online). doi:10.1007/s00158-008-0230-y

Acar E, Haftka RT, Sankar BV, Qui X (2006) Increasing allowable flight loads by improved structural modeling. AIAA J 44(2):376–381

Acar E, Haftka RT, Johnson TF (2007) Tradeoff of uncertainty reduction mechanisms for reducing structural weight. J Mech Des 129(3):266–274

Clarke SM, Griebsch JH, Simpson TW (2005) Analysis of support vector regression for approximation of complex engineering analyses. ASME J Mech Des 127(11):1077–1087

Dyn N, Levin D, Rippa S (1986) Numerical procedures for surface fitting of scattered data by radial basis functions. SIAM J Sci Statist Comput 7(2):639–659

Esat I (1999) Genetic algorithm-based optimisation of a vehicle suspension system. Int J Veh Des 21(2/3):148–160

Fang H, Solanki K, Horstemeyer M (2005) Numerical simulations of multiple vehicle crashes and multidisciplinary crashworthiness optimization. Int J Crashworthiness 10(2): 161–172

Goel T, Haftka RT, Shyy W, Queipo NV (2007) Ensemble of Surrogates. Struct Multidisc Optim 33(3):199–216

Gu L, Yang RJ, Tho CH, Makowski M, Faruque O, Li Y (2001) Optimization and robustness for crashworthiness of side impact. Int J Veh Des 25(4):348–360

Gunn SR (1997) Support vector machines for classification and regression. In: Image speech and intelligent systems research group, University of Southampton, Southampton

Hamza K, Saitou K (2004) Crashworthiness design using meta-models for approximating of box-section members. In: Proceedings of the 8th Cairo University international conference on mechanical design and production, Cairo, Egypt, vol 1, pp 591–602, 4–6 January

Horstemeyer M, Fang H, Solanki K (2004) Energy-based crashworthiness optimization for multiple vehicle impacts. Transportation 2004: Transportation and Environment, pp 11–16

Horstemeyer MF, Solanki K, Steele WG (2005) Uncertainty methodologies to characterize a damage evolution model. In: Plasticity 2005 conference, Kauai, Hawaii, 4–8 Jan

Ivanovic G (2000) The reliability allocation application in vehicle design. Int J Veh Des 24(2–3):274–286

Kaya N (2006) Optimal design of automotive diaphragm spring with fatigue resistance. Int J Veh Des 40(1/2/3):126–143

Kim H-S, Chen W, Wierzbicki T (2002) Weight and crash optimization of foam-filled three-dimensional "S" frame. Comput Mech 28:417–424

Kodiyalam S, Sobieszczanski-Sobieski J (2001) Multidisciplinary design optimisation - some formal methods, framework requirements, and application to vehicle design. Int J Veh Des 25(1/2):3–22

Kurtaran H, Eskandarian A, Marzougui D, Bedewi NE (2002) Crashworthiness design optimization using successive response surface approximations. Comput Mech 29:409–421

Lee K, Joo W, Song S, Cha I, Park G (2004) Optimization of an automotive side door beam, considering static requirement. In: Proceeding of the institution of mechanical engineers, part D. J Automobile Engineering 218:51–57

Lophaven SN, Nielsen HB, Søndergaard J (2002) DACE - a MATLAB kriging toolbox. In: Informatics and mathematical modelling, Technical University of Denmark, Lyngby

Martin JD, Simpson TW (2005) Use of Kriging models to approximate deterministic computer models. AIAA J 43(4): 853–863

Marvis D, Bandte O (1997) A probabilistic approach to multivariate constrained robust design simulation. SAE 97–5508

Mourelatos ZP, Kuczera RC, Latcha M (2006) An efficient Monte Carlo reliability analysis using global and local metamodels. In: Proceedings of 11th AIAA/ISSMO multidisciplinary analysis and optimization conference, September, Portsmouth, VA

Mullur AA, Messac A (2004) Extended radial basis functions: more flexible and effective metamodeling. In: Proceedings of 10th AIAA/ISSMO symposium on multidisciplinary analysis and optimization, Albany, NY, August 30–Sept 1

Myers RH, Montgomery DC (2002) Response surface methodology: process and product optimization using designed experiments. Wiley, New York

Piskie MA, Gioutsos T (1992) Automobile crash modeling and the Monte Carlo method. In: SAE technical paper series, pub. No. 920480. Society of Automotive Engineers, Warrendale

Qu X, Haftka RT, Venkataraman S, Johnson TF (2003) Deterministic and reliability-based optimization of composite laminates for propellant tanks. AIAA J 41(10):2029–2036

Qu X, Haftka RT (2004) Reliability-based design optimization using probabilistic sufficiency factor. Struct Multidisc Optim 27(5):314–325

Rais-Rohani M, Solanki K, Eamon C (2006) Reliability-based optimization of lightweight automotive structures for crashworthiness. In: 11th AIAA/ISSMO multidisciplinary analysis and optimization conference, Portsmouth, Virginia, 6–8 September, AIAA Paper 2006-7004

Rasmussen CE, Williams CKI (2006) Gaussian processes for machine learning. MIT, Cambridge

Robert CP, Casella G (2004) Monte Carlo statistical methods, 2nd edn. Springer, New York

Stander N, Roux W, Giger M, Redhe M, Fedorova N, Haarhoff J (2004) A comparison of metamodeling techniques for crashworthiness optimization. In: 10th AIAA/ISSMO multidisciplinary analysis and optimization conference, Albany, NY, 30 August-1 September, AIAA Paper No. 2004–4489

Sinha K (2007) Reliability-based multiobjective optimization for automotive crashworthiness and occupant safety. Struct Multidisc Optim 33(3):255–268

Sinha K, Krishnan R, Raghavendra D (2007) Multi-objective robust optimisation for crashworthiness during side impact. Int J Veh Des 43(1/2/3/4):116–135

Wang L, Basu PK, Leiva JP (2003) Design optimization of automobile welds. Int J Veh Des 31(4):377–391

Wang L, Beeson D, Wiggs G (2005) Gaussian process metamodels for efficient probabilistic design in complex engineering design spaces. In: ASME 2005 international design engineering technical conferences & computers and information in engineering conference, Long Beach, CA, September

Yang RJ, Tseng L, Nagy L, Cheng J (1994) Feasibility study of crash optimization. In: Gilmore BJ et al (eds) Advances in design automation DE 69(2):549–556.

Yang J, Hwang M, Sung T, Jin Y (1999) Application of genetic algorithm for reliability allocation in nuclear power plants. Reliab Eng Syst Saf 65:229–238

Yang RJ, Chuang C-H, Che X, Soto C (2000a) New applications of topology optimization in automotive industry. Int J Veh Des 23(1/2):1–15

Yang RJ, Gu L, Liaw L, Gearhart C, Tho CH, Liu X, Wang BP (2000b) Approximations for safety optimization of large systems. In: ASME design automation conference, Paper No: DETC-00/DAC-14245, Baltimore, MD, 10–13 September

Yang RJ, Gu L, Tho C, Choi KK, Youn BD (2002) Reliability-based design optimization of a full vehicle system. AIAA-2002-1758. In: Proc. 43rd AIAA SDM conference, Denver, CO

Youn BD, Choi KK, Yang RJ, Gu L (2004) Reliability-based design optimization for crashworthiness of side vehicle impact. Struct Multidisc Optim 26:272–283

Zaouk AK, Marzougui D, Bedewi NE (2000a) Development of a detailed vehicle finite element model, Part I: methodology. Int J Crashworthiness 5(1):25–35

Zaouk AK, Marzougui D, Kan CD (2000b) Development of a detailed vehicle finite element model, Part II: material characterization and component testing. Int J Crashworthiness 5(1):37–50